

High spatial resolution Hall nano-sensors by tuned direct-write Co/C-FEBID

M. S. Gabureac^{*}, L. Bernau^{*}, G. Boero^{**} and I. Utke^{*}

^{*}Swiss Federal Laboratories for Materials Science and Technology (EMPA),
Feuerwerkerstr. 39, CH-3602 Thun, Switzerland, mihai.gabureac@empa.ch

^{**}Swiss Federal Institute of Technology at Lausanne (EPFL), CH-1015 Lausanne, Switzerland

ABSTRACT

Gas assisted focused electron beam induced deposition is a direct write technique that allows for the deposition of nanoscale structures inside standard scanning electron microscopes. Here we show that the composition of the nano-deposits can depend on their size, which can be used as an additional parameter, besides the control of the beam dwell time, in order to tune the metal/matrix ratio and to obtain new nanoscale materials with tailored properties. By optimizing the Cobalt/Carbon ratio and the size of the active area, it was possible to obtain superparamagnetic Hall sensors with outstanding magnetic spatial resolution. These sensors have been successfully used for detecting single paramagnetic micro-beads commonly used as labels in biological and medical research.

Keywords: focused electron beam induced deposition, composition tuning, nanocomposite magnetic nanosensors, micromagnetic bead detection, bio-nanosensors.

1 INTRODUCTION

The gas assisted focused electron or ion beam (FEB/FIB) induced deposition is a small, minimally invasive, direct write technique which allows for the deposition of 2D and 3D nanoscale structures inside standard scanning electron microscopes (SEM) [1-3]. Depending on the size of the charged particle beam, deposits of only a few nanometers in lateral size are possible [4], making this technique suitable for nanoprototyping.

Although it allows for the deposition of a large choice of materials (precursor choice similar to CVD), in the case of metals, the FEBID technique is still in the quest for high purity deposits similar to those routinely obtained by standard depositions techniques [5]. While the deposition of high purity metals is sometimes possible even when using organo-metallic precursors [6, 7] (depending significantly on the autocatalytic properties of the deposited metal), in general, the result is a granular deposit formed by a mixture of the desired metal surrounded by a matrix with different composition.

This is the result of different processes such as partial decomposition of the original precursor, co-deposition of ligands or their decomposed parts, co-deposition of carbon from background pressure or even contamination molecules from the substrate [8]. The resulting FEBID co-deposition process can be modeled using a two adsorbate model which

also describes the control of the composition, when the adsorbed molecules have different properties (selective depletion) [9].

Here we show that it is possible to control the composition of the FEBID deposits not only by carefully tuning the beam parameters (dwell times), but also by varying the size of deposits that can play a crucial role and should be taken into account as an extra parameter when tuning the Metal:Matrix ratio. The precursor used was the cobalt carbonyl which allowed for the in-situ direct fabrication of a magnetic nano-composite material consisting of metal nanoparticles embedded in a carbonaceous matrix. We show that Langevin analysis of the Hall Voltage can be used in order to determine the magnetic characteristics of the nanocomposite deposits [10].

From the magnetic characterization we conclude that the Extraordinary Hall effect is amplified in the nanocomposite structure when the metal composition is decreasing. We show that Hall sensors with concentrations around 70% and sizes below 100 nm have a high magnetic spatial resolution, which allows for detection of single paramagnetic beads.

2 NANOFABRICATION

The FEBID experiments were done in a Hitachi S3600 SEM equipped with a tungsten thermal emission filament. The pumping system consists of an oil diffusion pump back-pumped by an oil roughing pump. This results in a base pressure of approximately 1×10^{-5} mbar with a particular fingerprint of hydrocarbons in the background pressure. The precursor used was the cobalt carbonyl ($\text{Co}_2(\text{CO})_8$) (Ar stabilized, CAS 10210-68-1), supplied from an internal reservoir placed at about 100 μm high and 100 μm away from the beam axis at an angle of about 40° with respect to the substrate surface. The precursor flux during the experiments was about 4.4×10^{15} molecules/s, as estimated from mass loss measurements. According to our gas flow Monte Carlo simulations, this translates into 1.5×10^{17} molecules/cm²/s impinging on the irradiated spot.

We have used the XENOS lithography system to control the electron beam during deposition. The deposition control parameters are the nominal dwell time t_d , i.e. the time the beam irradiates a pixel before moving to the next, the inter-pixel distance, defined as the distance between two adjacent pixels irradiated by the beam, and the refresh time t_r , which measures the time elapsed before the next iteration of the structure irradiation. Dividing the total irradiation time by the total exposed surface yields the deposition dose in

C/cm^2 . In our experiments, the total deposition dose was kept constant to $10 \text{ C}/\text{cm}^2$ and the refresh time was always kept $\geq 10 \text{ ms}$, to ensure full replenishment with precursor molecules between two irradiation iterations.

We present here two different experiments that allowed to controllably tune the metal:carbon ratio of the Co-FEB deposits. The deposits were characterized with regard to the composition using energy dispersive x-ray spectroscopy (EDX), using a 3 keV probe. The accuracy of the compositional values obtained by this mean was checked to be correct within $\pm 5 \text{ at.\%}$ by calibration measurements on Cobalt-carbonate (CoCO_3).

2.1 Composition tuning by control of width

In the first experiment we have fabricated seven $20 \mu\text{m}$ long lines with different widths using a 25kV, 10 nA, beam current (beam size estimated around 200 nm) and a dwell time of $2 \mu\text{s}$ per pixel. The total dose was fixed to $10 \text{ C}/\text{cm}^2$ while the pitch (distance between consecutive pixels) was of 4 nm. The optimized beam scanning strategy was a meander fill allowing for the full replenishment with the $\text{Co}_2(\text{CO})_8$ between consecutive lines. Both the dwell time and the refresh time per line were fixed for all deposits, as well as the number of pattern repetitions/total dose. The only parameter that varied was the width.

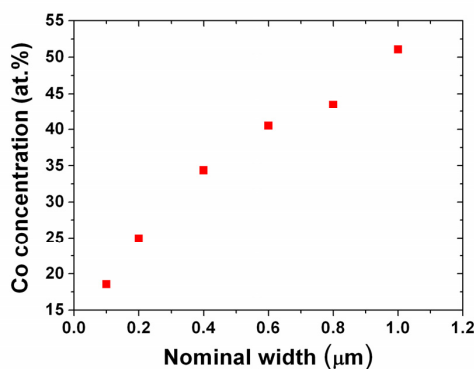


Figure 1: Dependence of Cobalt concentration on the width for $20 \mu\text{m}$ long Co-FEBID lines on Au, for a 10 nA, 25 kV beam, $2 \mu\text{s}/\text{pixel}$ dwell time, 4 nm pitch, $10 \text{ C}/\text{cm}^2$ dose, $1 \times 10^{-5} \text{ mbar}$ pressure and refresh time larger than 776 ms.

As we have recently shown [9], the purity of the FEBID nano-deposits depends not only on the efficiency of decomposition of the precursor molecule, but also on the *co-deposition of carbon*. Since the carbon is not directly injected on the irradiation spot, surface diffusion can be an important mechanism contributing to the total amount of carbon available for deposition. Because the deposition starts on the contours of the structure, the carbon source is

depleted and the amount of carbon arriving inside the deposition area will depend on the total time needed to close one contour. This provides a second mechanism for tuning the deposit composition and that can be understood using the dual adsorbate FEB co-deposition model. This was confirmed experimentally, as shown in Figure 1, where the metal concentration increased linearly with the width.

2.2 Composition tuning by dwell time

In the second experiment we present Hall sensors (square active area connected by contact lines) where the composition was tuned by using different beam dwell times. The inter-pixel distance was set to 30 nm. This compares to a beam diameter (FWHM) estimated to 70 nm (assessed experimentally using BeamMetr), for 25 kV acceleration voltage and 1 nA beam current.

Because the adsorbed hydrocarbon molecules are depleted much faster than the $\text{Co}_2(\text{CO})_8$, we were able to fabricate Hall nano-sensors with a large variation of Cobalt concentrations in a time window between $0.5 \mu\text{s}$ and $50 \mu\text{s}$, as shown in Figure 2.

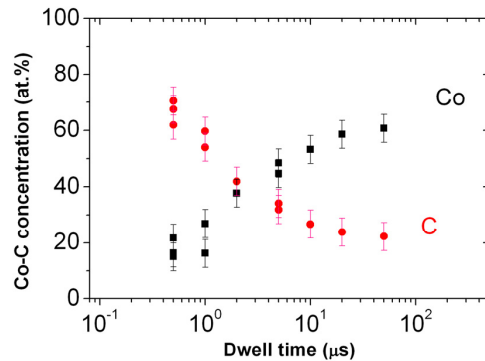


Figure 2: EDX analysis of Co/C at.% for FEBID deposits with controlled tuning of the dwell time. The Co:C concentration variation in the $500 \text{ ns} - 50 \mu\text{s}$ dwell time interval is consistent with the two-adsorbate model described in reference [9].

3 MAGNETIC PROPERTIES OF NANOCOMPOSITE CO-C HALL SENSORS

The magnetic properties of FEB nanocomposite deposits are determined by the nanoparticle size and their spacing. When particle sizes are of only a few nanometers and the concentration is below the percolation threshold, the deposits are superparamagnetic and exhibit the Giant Hall effect, an exponential increase in the magnetic sensitivity as the metal concentration decreases [10].

The nanoparticle size can be estimated using Langevin analysis of the Hall signal of the FEB nano-sensors as shown in [10] for Co-C deposits. Because the nano-deposits are superparamagnetic, the Hall sensors are linear in zero field, making them suitable for the detection of very low magnetic fields. Another remarkable property of these nanocomposite deposits is the fact that their magnetic sensitivity is increasing exponentially when the metal concentration is decreasing, as shown in Figure 3.

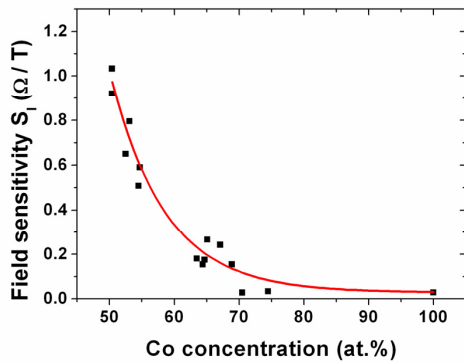


Figure 3: Exponential increase in the magnetic field sensitivity when the Co concentration is approaching the M-I transition as explained in [10].

The Hall Voltage measurement on these deposits allowed for the optimization of the magnetic properties in view of their use for the detection of the single paramagnetic beads. In Table 1 we show the magnetic characteristics of different types of Hall sensors classified with respect to their ability to detect the smallest change in the magnetic flux (Φ_{\min}/Φ_0). The Co-C sensors perform better than the pure Co sensors but they also outperform the highest sensitivity semiconducting Hall sensors. This is because the active area can be reduced below 100 nm and because the composition tuning also allows for the optimization of the resistivity/detection current flowing in the device. The combination of high spatial resolution and the flexibility of the FEBID technique, allows for these sensors to be easily integrated on chip and to be used as bio-nano-sensors or for Scanning Hall Probe Microscopy.

Sensor type	InAs	InGaAs	n-Si	Co	FePt	Bi	InSb	InAsSb	Co-C
Width (nm)	1000	2000	2400	100	160	50	500	1000	100
$S_l (\Omega/T)$	616	700	175	0.03	325	4	-	2750	0.15
B_{\min} (nT/Hz ^{1/2})	4300	400	200	50000	166000	80000	720	51	900
Φ_{\min}/Φ_0	2×10^{-3}	2×10^{-4}	5.5×10^{-4}	2.5×10^{-4}	1.6×10^{-4}	10^{-4}	9×10^{-5}	2.5×10^{-5}	5×10^{-6}

Table 1: Magnetic properties comparison for different types of sensors: although the Co-C Hall sensor has worse magnetic sensitivity (S_l) and field resolution (B_{\min}), its magnetic spatial resolution Φ_{\min}/Φ_0 is the better because of its higher conductivity and scalable properties when the active area is reduced below 100 nm where $\Phi_0 = h/(2e)$ is the magnetic flux quantum [10].

4 DETECTION OF A SINGLE PARAMAGNETIC MICROBEAD

Paramagnetic beads, used as markers in drug screening or in DNA manipulation, or patterned magnetic nanostructures, used in perpendicular magnetic recording, can be assimilated to dipolar field sources producing highly localized, spatially inhomogeneous magnetic fields [11, 12]. Therefore, sensors with high spatial resolution are needed in order to detect such small magnetic objects, in the micrometer or nanometer size range.

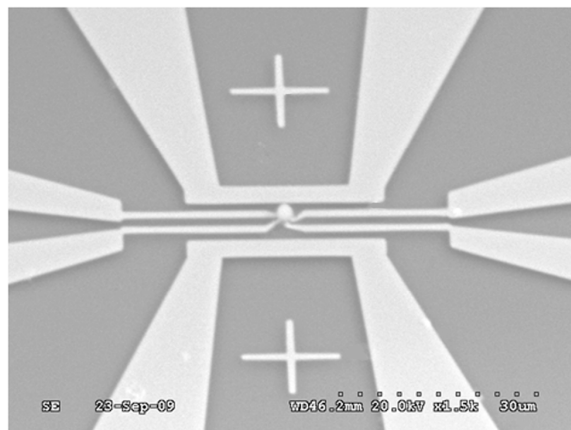


Figure 4: Superparamagnetic Dynabead M-270 from Dynal positioned above a Co-FEBID Hall nano-sensor

Here we report the detection of a single paramagnetic bead (M-270, 2.8 μm in diameter, streptavidin coated, Dynabead from Dynal), placed above the Hall sensor by *in situ* nano-manipulation, using only an AC magnetic field perpendicular to the sensor plane. The bead was placed on the active area of the Hall sensor (position ON in Figure 5) using an AFM tip and then it was picked up and moved away from the sensor (position OFF). The Hall signal was recorded *in situ* before the bead was on, then with the bead on and then again when the bead was removed. The difference in the Hall voltage with the bead on/off is shown in Figure 5. The AC magnetic signal was decomposed in two components, one in phase and the other one out of phase with respect to the electromagnetic induced signal by the external AC field by using a Lock-in amplifier

The separation of the magnetic signal was done for each position of the bead when no DC current is flowing through the sensor. When the DC current was turned on, the Hall signal generated by the external field was detected as being out of phase with respect to the induced e.m. voltage. The Hall signal generated by the magnetic field of the bead is then added as an extra component of the Hall voltage.

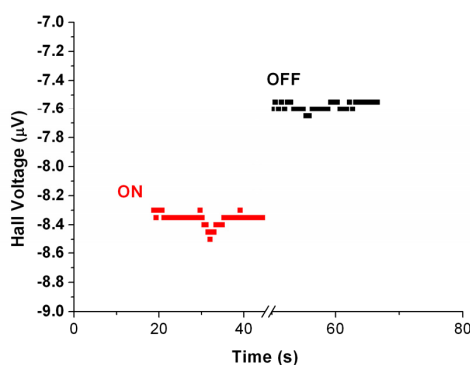


Figure 5 Detection of a single paramagnetic bead showing different Hall Voltages when the bead is on top of the sensor (position ON) and when it is removed in situ from the sensor (position OFF).

The Hall voltage induced by the AC field when the bead was off was $7.5 \mu\text{V}$, proportional with the DC current and AC field, and increased by 800 nV with the bead on top of the sensor. The DC current used was 15 mA . The inductive signal generated by external the AC coils was of $716 \mu\text{V}$ at 17.2 Hz and was separated from the Hall signal for each bead position. The signal to noise ratio can be improved significantly by reducing the electromagnetic induced signal, for example if on chip current lines are used to generate a local AC field, as shown in Figure 4.

5 CONCLUSIONS

We have used focused electron beam induced deposition to fabricate nanocomposite Hall nanosensors with different Co:C ratios. The controlled tuning of the composition was realized by two methods based on the two adsorbate FEB co-deposition model and selective depletion of carbon: by controlling the size (width) of the deposits.

The magnetic properties of the nanocomposite material were studied using Langevin analysis of the voltage produced by FEB Hall sensors with different compositions. The minimum detectable magnetic flux change compares favorably with respect to the other types of magnetic nanosensors. This allowed for the detection of a single paramagnetic bead opening the way for the integration of these sensors on lab-on-a-chip devices for biological and medical applications.

Acknowledgements:

We thank for the financial support from the European Commission in the 7th Framework Programme (Project FAB2ASM, Grant Agreement n°260079) and the CTI (Project No.: 10710.1 PFNM-NM).

REFERENCES

- [1] I. Utke, and A. Gölzhäuser, "Small, Minimally Invasive, Direct: Electrons Induce Local Reactions of Adsorbed Functional Molecules on the Nanoscale", *Angewandte Chemie International Edition*, 49, 9328-9330, 2010.
- [2] I. Utke, P. Hoffmann, and J. Melngailis, "Gas-assisted focused electron beam and ion beam processing and fabrication", *Journal of Vacuum Science & Technology B*, 26, 1197-1276, 2008.
- [3] W. F. van Dorp, and C. W. Hagen, "A critical literature review of focused electron beam induced deposition", *Journal of Applied Physics*, 104, 081301-42, 2008.
- [4] K. Furuya, "Nanofabrication by advanced electron microscopy using intense and focused beam", *Science and Technology of Advanced Materials*, 9, 014110, 2008.
- [5] A. Botman, J. J. L. Mulders, and C. W. Hagen, "Creating pure nanostructures from electron-beam-induced deposition using purification techniques: a technology perspective", *Nanotechnology*, 20, 372001 (17pp), 2009.
- [6] A. Fernandez-Pacheco *et al.*, "Magnetotransport properties of high-quality cobalt nanowires grown by focused-electron-beam-induced deposition", *Journal of Physics D: Applied Physics*, 42, 055005 (6pp), 2009.
- [7] T. Lukasczyk *et al.*, "Electron-Beam-Induced Deposition in Ultrahigh Vacuum: Lithographic Fabrication of Clean Iron Nanostructures", *Small*, 4, 841-846, 2008.
- [8] J. J. Hren, "Specimen Contamination in Analytical Electron Microscopy: Sources and Solutions", *Ultramicroscopy*, 2, 375-380, 1979.
- [9] L. Bernau *et al.*, "Tunable Nanosynthesis of Composite Materials by Electron-Impact Reaction", *Angewandte Chemie International Edition*, 49, 8880-8884, 2010.
- [10] M. S. Gabureac *et al.*, "Granular Co-C nano-Hall sensors by focused-beam-induced deposition", *Nanotechnology*, 21, 115503 (5pp), 2010.
- [11] M. Gabureac *et al.*, "Focused Ion and Electron Beam induced deposition of magnetic nanostructures", Oxford University Press, 2011, 9780199734214.
- [12] P. A. Besse *et al.*, "Detection of a single magnetic microbead using a miniaturized silicon Hall sensor", *Applied Physics Letters*, 80, 4199-4201, 2002.